



HAL
open science

Wireless electrodynamic power transfer: modeling and discussion of a dual-mode receiver

Adrien Ameye, Adrien Morel, Rémi Recoquillé, Nicolas Garraud, Pierre Gasnier, Adrien Badel

► **To cite this version:**

Adrien Ameye, Adrien Morel, Rémi Recoquillé, Nicolas Garraud, Pierre Gasnier, et al.. Wireless electrodynamic power transfer: modeling and discussion of a dual-mode receiver. PowerMEMS 2024 - IEEE 23rd International Conference on Micro and Miniature Power Systems, Self-Powered Sensors and Energy Autonomous Devices, Nov 2024, Tonsberg, Norway. pp.2-5, 10.1109/PowerMEMS63147.2024.10814423 . hal-04867097

HAL Id: hal-04867097

<https://hal.science/hal-04867097v1>

Submitted on 6 Jan 2025

HAL is a multi-disciplinary open access archive for the deposit and dissemination of scientific research documents, whether they are published or not. The documents may come from teaching and research institutions in France or abroad, or from public or private research centers.

L'archive ouverte pluridisciplinaire **HAL**, est destinée au dépôt et à la diffusion de documents scientifiques de niveau recherche, publiés ou non, émanant des établissements d'enseignement et de recherche français ou étrangers, des laboratoires publics ou privés.

WIRELESS ELECTRODYNAMIC POWER TRANSFER: MODELING AND DISCUSSION OF A DUAL-MODE RECEIVER

Adrien Ameye¹, Adrien Morel¹, Rémi Recoquille^{1,2}, Nicolas Garraud², Pierre Gasnier² and Adrien Badel¹
¹SYMME, Univ. Savoie Mont Blanc, Annecy, FRANCE and
²CEA-Leti, Univ. Grenoble Alpes, FRANCE

ABSTRACT

This paper investigates the dynamics of an electrodynamic receiver based on a rotating permanent magnet, incorporating a magnetic stiffness to enable operation in both oscillating and continuously rotating modes. The aim of this dual-mode system is to operate efficiently and robustly with both high- and low- excitation field amplitudes. The behaviour of the proposed receiver has been simulated using parameters identified from a prototype to determine the necessary conditions for operation in each of the two modes. Finally, we discussed various transition strategies that enable switching from the oscillating mode to the continuously rotating mode.

KEYWORDS

Electrodynamic wireless power transfer, distant charging, dual mode, nonlinear dynamics.

INTRODUCTION

Context

In the last few years, electrodynamic wireless power transfer (EWPT), based on a moving magnet in the receiver (Fig. 1), has been proposed as an alternative to inductive wireless power transfer for being sensitive to very low frequency magnetic fields (10 Hz -1000 Hz). The use of low frequencies improves transmission efficiency through conductive media, reduces EMI and limits human exposure to high-frequency emission fields.

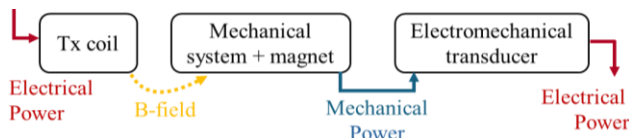


Figure 1: Energy chain of an electrodynamic WPT system.

Operating modes

Among the variety of receiver topologies proposed in the literature, the ones based on rotating magnets are compact and exhibit high power-density. Presently, there are two dominant modes for rotational EWPT devices:

- **The oscillating mode**, characterized by an alternating rotation of the magnet around its stable position (Fig. 2A)[1]. This mode requires a restoring torque, i.e. a rotational stiffness. Such mode benefits from high-quality factors making it sensitive to weak magnetic fields but is limited to low power densities (Fig.3).
- **The continuously rotating mode**, in which the magnet makes complete rotations (Fig. 2B) [2]. This mode offers superior power density (Fig. 3) and eliminates wear-prone deformable parts, but requires a substantial magnetic field amplitude and gradual acceleration to initiate operation [3].

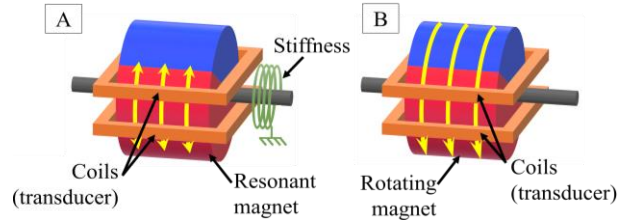


Figure 2: Representation of the two operating modes: oscillating and continuously rotating device.

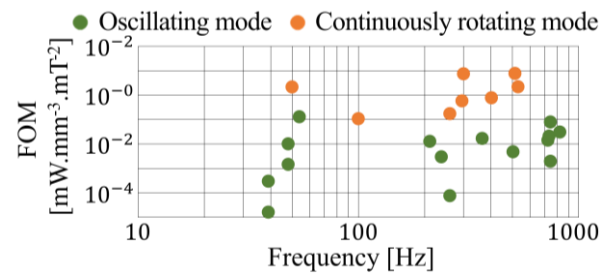


Figure 3: Power density of rotational EWPT [to be published].

Because the oscillating mode is very sensitive to low fields, and since the continuously rotating mode is more advantageous in terms of power density, we propose to study the dynamics of a dual-mode receiver capable of operating in both modes depending on the field conditions. First, we outline a model of the system. Next, we analyse the receiver's performance in both operational modes. Finally, we explore potential strategies for transitioning between oscillating and rotation modes.

SETUP AND MODEL

The receiver used in this study is based on a 0.83 cm³ generator previously introduced [4]. It consists in a diametrically magnetized magnet that rotates freely around its axis, with a coil wound around the magnet as an electromechanical transducer (Fig. 4A-B). To introduce a stiffness required for the oscillating mode, a secondary permanent magnet is fixed close to the rotating magnet (Fig. 4C). The receiver is connected to a variable resistive load.

The model introduced in [3] is used to describe the mechanical dynamics of the receiver:

$$\tau = J\ddot{\theta} + K\theta + D_{eq}\dot{\theta} \quad (1)$$

In this equation, τ is the excitation torque applied on the permanent magnet by the time varying magnetic field:

$$\tau = mB_0 \sin(\theta) \sin(\omega t) \quad (2)$$

with B_0 the field amplitude, and m the magnetic moment of the magnet.

$K\theta$ is the torque applied by the constant equivalent magnetic field B_S from the stiffening magnet:

$$K = \frac{m B_S \cos(\theta)}{\theta} \quad (3)$$

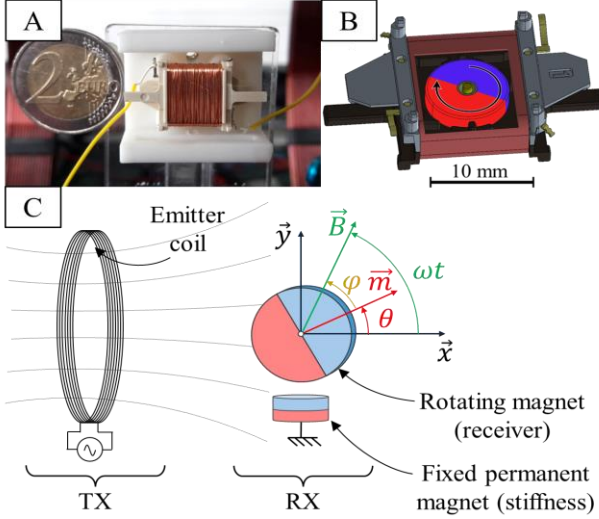


Figure 4: A-B. Picture and representation of the integrated EWPT. C. Schematic of the system set up with the stiffener made from a permanent magnet.

$D_{eq} = D + D_e$ is the equivalent damping comprising both electrically-induced damping D_e and mechanical damping D . Other parameters used and their identified values are summarized in Table 1.

Table 1: Measured parameters of the EWPT receiver.

Sy.	Description	Value	Unit
θ	Angular position of the rotating magnet (Fig. 4C)		[rad]
R_l	Electrical load resistance		$[\Omega]$
J	Rotational inertia	$8.1e^{-9}$	$[\text{kg m}^2]$
m	Magnetic moment	0.12	$[\text{A} \cdot \text{m}^2]$
D	Mechanical damping coefficient	5.2	$[\text{nNm/s}]$
R_c	Rx coil internal resistance	114	$[\Omega]$
β	Transduction coefficient	10.2	$[\text{mNm/A}]$

The mechanical equation (1) can be reformulated by introducing three characteristic system pulsations, denoted ω_{lim} , ω_r , and ω_B :

$$\ddot{\theta} + \omega_r^2 \cos(\theta) = \omega_B^2 \left(\sin(\theta) \sin(\omega t) - \frac{\dot{\theta}}{\omega_{lim}} \right) \quad (4)$$

$\omega_r = \sqrt{mB_S/J}$ is the resonance pulsation at small angles, $\omega_{lim} = D_{eq}/J$ is the cut off pulsation ie. pulsation beyond which the forces, due to losses, prevent the existence of continuously rotating mode [3], and $\omega_B = \sqrt{mB_0/J}$ is a pulsation related to the excitation amplitude, which has been empirically determined in this work.

Finally, it can be proven that the average electrical power P is expressed as follows [3]:

$$P = \frac{1}{2} \beta^2 \frac{R_c}{(R_c + R_l)^2} \dot{\theta}^2 \quad (5)$$

The performance of our system in the two operating modes has been estimated by simulations using Matlab Simulink. These results were validated with experimental measurements for the continuously rotating mode with a progressive frequency sweep of the magnetic field. Fig. 5 shows a good correspondence between the measurements and simulations for excitation frequencies below 550 Hz.

A minimum field strength of 0.4 mT is required for the continuously rotating mode. The system supplies 63 mW at 0.8 mT, reaching up to 240 mW at 2 mT.

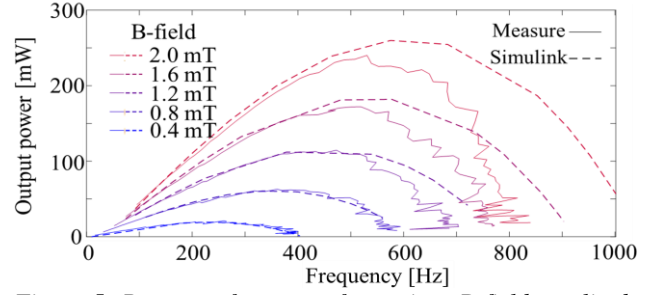


Figure 5: Power vs frequency for various B-field amplitude continuously rotating mode (without magnetic stiffness).

Fig. 6 shows simulated power output in oscillating mode for different excitation field amplitudes with a stiffness field of $B_S = 12.8$ mT.

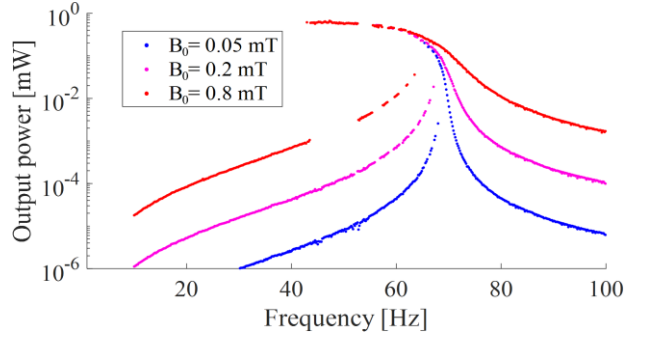


Figure 6: Simulated output power versus frequency for various B-field amplitude in oscillating mode ($B_S = 12.8$ mT).

In oscillating mode, a strong nonlinear softening effect, attributed to the nonlinear magnetic stiffness, is observed. The output power in oscillating mode, estimated at 0.66 mW for 0.8 mT, is significantly lower (100 \times) than in continuously rotating mode and is obtained at lower frequencies (~ 45 Hz). However, at lower field strengths, the continuously rotating mode cannot be exploited, whereas the oscillating mode generates 0.20 mW at 0.05 mT and 0.58 mW at 0.2 mT.

STUDY OF SYSTEM DYNAMICS

In this section, we aim to identify the necessary conditions for achieving both operating modes. Two simulations were performed by varying initial conditions (phase and initial rotation speed) and the emitter frequency within a system without ($\omega_r = 0$ rad/s) and with stiffness ($\omega_r = 3\omega_B$) (Fig. 7).

When the receiver operates without magnetic stiffness (Fig. 7A), three behaviours can be identified:

- For $\omega < \omega_B$, the system exhibits a complex and aperiodic dynamic. The inertia is insufficient relative to the excitation torque for the rotating magnet to follow a periodic trajectory in phase space. Nevertheless, up to 100 μ W can be extracted.
- For $\omega_B < \omega < \omega_{lim}$, two solutions coexist depending on initial conditions. A first solution corresponds to continuous rotation ($\dot{\theta} = \pm\omega$), which is achievable when the system is pre-launched. The second solution corresponds to the magnet remaining stationary ($\dot{\theta} = 0$, stabilizing around $\theta = \{0, \pi\}$), with no output power.

Both cases are observed experimentally.

- Finally, for $\omega > \omega_{lim}$, only the solution $\dot{\theta} = 0$ exists, and no power can be extracted.

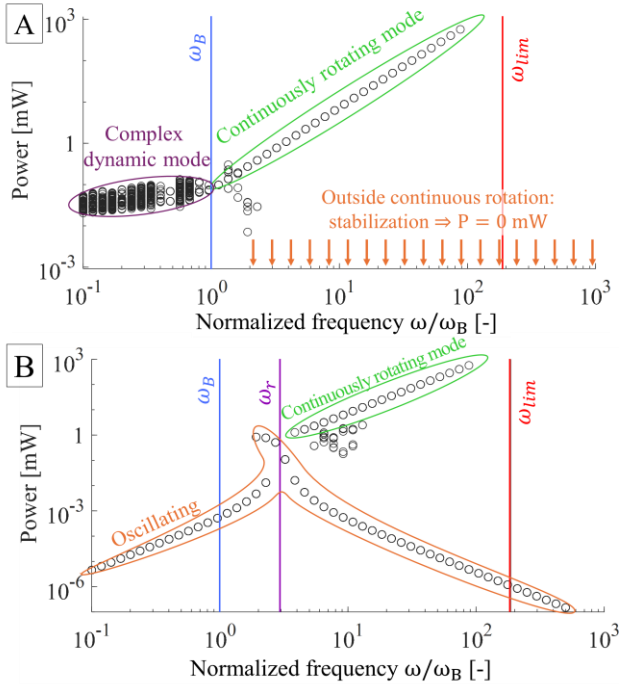


Figure 7: Simulations of the output power versus normalized frequency ω/ω_B . A: for a system without stiffness ($K=0$). B: for a system with stiffness ($\omega_r = 3\omega_B$).

By adding a magnetic stiffness (Fig. 7B), the receiver dynamics shows different types of behaviours:

- For $\omega < \omega_r$, the system behaves as a resonant system, oscillating around an equilibrium position $\theta = \pi/2$. The output power is low away from resonance, and increases significantly, reaching 0.6 mW near $\omega = \omega_r$. The complex dynamic mode no longer exists.
- For $\omega_r < \omega < \omega_{lim}$, both modes coexist: the continuous rotation providing high output power, and the oscillating mode offering lower non-zero power.
- For $\omega > \omega_{lim}$, the system behaves like a resonant system far from the resonance frequency with very low output power (<10 's of μW).

From this analysis, the several conclusions are drawn:

- The complex dynamic mode occurs when the stiffness is lower than the excitation ($\omega_r < \omega_B$) and for excitation frequencies $< \omega_B$.
- The oscillating mode exists if stiffness is applied to the system. It occurs for excitation frequencies $\omega > \omega_B$ if $\omega_r < \omega_B$, or at any excitation frequency if $\omega_r > \omega_B$.
- The continuously rotating mode is only accessible for frequencies $\omega \in [\omega_B, \omega_{lim}]$ when $\omega_r < \omega_B$, and similarly for $\omega \in [\omega_r, \omega_{lim}]$ when $\omega_r > \omega_B$.
- Finally, when no stiffness is applied to the system, it stabilizes around a fixed point for $\omega > \omega_B$.

TRANSITION TO CONTINUOUSLY ROTATING MODE

In the previous section, we observed that both modes can co-exist for some forcing amplitude and frequency. In simulation, the operation mode of the receiver is determined

by the initial condition of the magnet. However, in practice, the receiver will most of time operates in its lowest power mode which is usually the most stable one. In this section, we investigate several strategies for transitioning from the low-power oscillating mode to the high-power continuously rotating mode. Based on the conditions discussed earlier, three methods can be implemented.

Transition through the complex dynamic mode

The first method involves gradually increasing the excitation frequency for systems with no stiffness (Fig. 9). The excitation frequency is initially lowered below the pulsation ω_B , ensuring to operate in the complex dynamic mode. A gradual increase in the excitation frequency then allows the magnet to accelerate while following the continuously rotating mode.

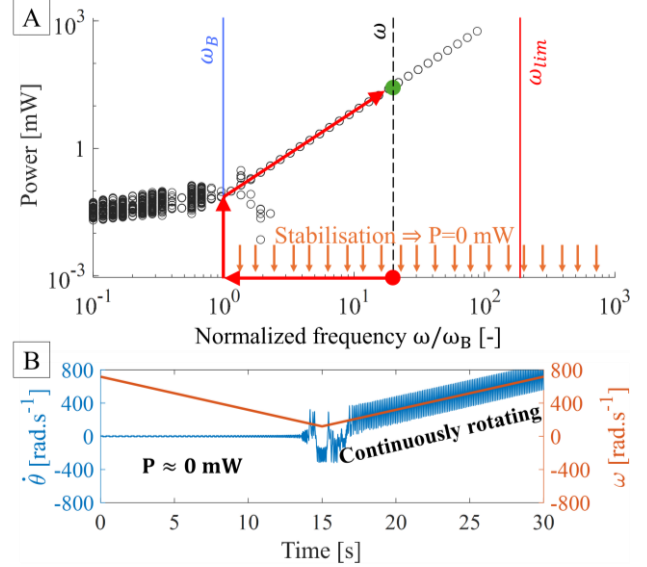


Figure 9: Transition strategy to continuously rotating mode with a jump through $\omega = \omega_B$ for a system **with no stiffness**. A. Power versus frequency graph, with red and green dots for initial and target states. B. Time simulation of the transition strategy.

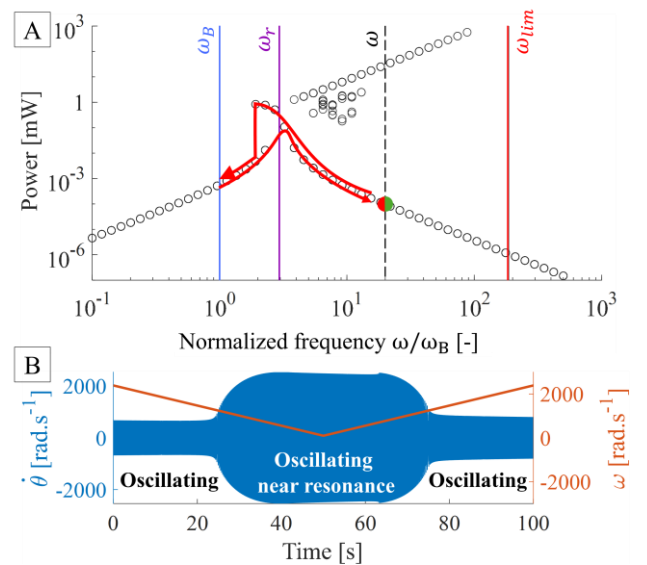


Figure 10: Transition strategy to continuously rotating mode by passing through $\omega = \omega_B$ for a system with stiffness ($\omega_r = 3\omega_B$). A. Power versus frequency graph. B. Time simulation of the transition strategy.

This method is feasible in the absence of stiffness (Fig. 9A), as the orbit corresponding to stabilization around a fixed point only appears for frequencies $\omega > \omega_B$. Therefore, lowering the excitation frequency forces the system into a higher energy orbit. A time-based simulation of this method is presented in Fig. 9B.

For systems with stiffness, the complex dynamic mode is no longer present, and the oscillating mode corresponds to a lower energy state, which does not allow a transition to the continuously rotating mode (Fig. 10A). Lowering the excitation frequency, followed by increasing it from $\omega = \omega_B$, no longer enables the system to reach the continuously rotating mode, as shown by the time-based simulation (Fig. 10B).

Transition by increasing the field intensity

The second method involves temporarily increasing the excitation amplitude B_0 so that the pulsation ω_B becomes greater than the pulsation ω_r and matches the excitation frequency ω (Fig. 11A), allowing the system to enter complex dynamic mode. A time-based simulation of this solution for a system with stiffness is presented in Fig. 11B, the amplitude B_0 being increased over half an excitation period ($B_{0,pulse} = 11 \cdot B_0$).

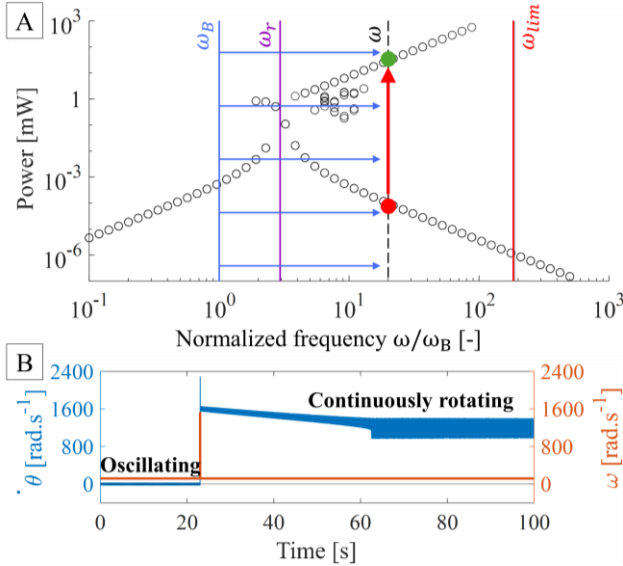


Figure 11: Transition strategy to continuously rotating mode by briefly increasing B-field for a system with stiffness ($\omega_r = 3\omega_B$). A. Power versus frequency. B. Time simulation of the transition strategy.

Depending on the operating frequency, this method may require a significant increase in the excitation field. Although the time needed for the transition may be short, regulatory limits and transmitter design constraints can limit the ability to generate such strong magnetic fields. The minimum excitation amplitude can be determined from equation (6):

$$\omega_B = \omega \Rightarrow B_{0,pulse} = \omega^2 J / m \quad (6)$$

Use of the resonant frequency

A final method involves using the oscillating mode at resonance to store enough energy and then transferring it to the rotating magnet via the electromechanical transducer (Fig. 12). This method, has already been proposed for multi-stable systems in the context of energy harvesting [5]. Since the continuously rotating mode is not accessible at $\omega = \omega_r$, it

requires an increase in excitation frequency. Therefore, communication between the receiver and the transmitter is necessary for this approach.

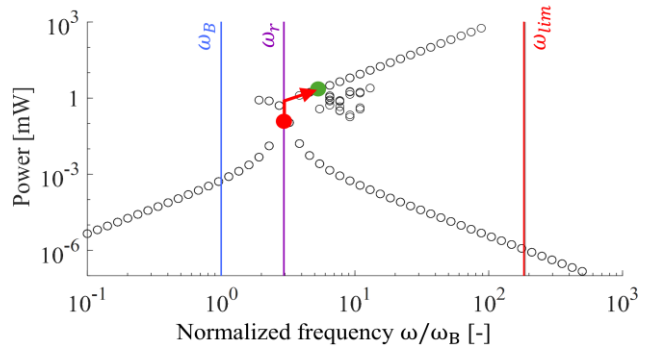


Figure 12: Transition strategy to continuously rotating mode using resonance frequency in the power vs. frequency graph.

CONCLUSION

In this study, we introduced an Electromagnetic Wireless Power Transfer (EWPT) receiver capable of operating in two modes: oscillating mode and continuously rotating mode. After presenting a brief analytical model and demonstrating the performance of our system in both operational modes, we found that continuously rotating mode delivers significantly higher output power, while oscillating mode can still provide low output power even under weak excitation fields.

Utilizing our model to gain insights into the conditions required to operate in these two modes, we explored and simulated strategies for transitioning from the oscillating mode, which yields less energy, to the continuously rotating mode, offering greater energy output.

The next step will involve applying analytical tools to rigorously confirm our findings and implementing these transitions on the real system.

ACKNOWLEDGEMENTS

This work was conducted as part of the strategic scientific collaboration between SYMME-USMB and CEA-Leti.

REFERENCES

- [1] S. Smith et al., 'Dual-Transduction Electromechanical Receiver for Near-Field Wireless Power Transmission', MEMS 2021, Jan. 2021, doi: 10.1109/MEMS51782.2021.9375416.
- [2] Y. Wu et al., 'Low-Frequency Wireless Power Transfer Via Rotating Permanent Magnets', IEEE Transactions on Industrial Electronics, Oct. 2022, doi: 10.1109/TIE.2022.3158010.
- [3] N. Garraud et al., 'Modeling and experimental analysis of rotating magnet receivers for electrodynamic wireless power transmission', J. Phys. D: Appl. Phys., Feb. 2019, doi: 10.1088/1361-6463/ab0643.
- [4] A. Ameye et al., '0.83-cm³ 240-mW electrodynamic wireless power receiver', in JNRSE 2023, Jun. 2023. Available: <https://hal.univ-smb.fr/hal-04172968>
- [5] C. Saint-Martin et al., 'Optimized and robust orbit jump for nonlinear vibration energy harvesters', Nonlinear Dyn, Mar. 2024, doi: 10.1007/s11071-023-09188-x.

CONTACT

*A. Ameye, tel: +334 500 965 67; adrien.ameye@univ-smb.fr